Journal of Zhejiang University-SCIENCE B (Biomedicine & Biotechnology) in press
www.jzus.zju.edu.cn; www.springer.com/journal/11585
E-mail: jzus_b@zju.edu.cn

Research Article

https://doi.org/10.1631/jzus.B2300777

Promising protective treatment potential of endophytic bacterium *Rhizobium aegyptiacum* for ulcerative colitis in rats

Engy ELEKHNAWY[1*]✉, Duaa ELIWA[2*], Sebaey MAHGOUB[3], Sameh MAGDELDIN[3,4], Ehssan MOGLAD[5], Sarah IBRAHIM[6], Asmaa Ramadan AZZAM[6], Rehab AHMED[7,8], Walaa A. NEGM[2]✉

[1]*Pharmaceutical Microbiology Department, Faculty of Pharmacy, Tanta University, Tanta 31527, Egypt*
[2]*Department of Pharmacognosy, Faculty of Pharmacy, Tanta University, Tanta 31527, Egypt*
[3]*Proteomics and Metabolomics Research Program, Department of Basic Research, Children's Cancer Hospital 57357, Cairo 11441, Egypt*
[4]*Department of Physiology, Faculty of Veterinary Medicine, Suez Canal University, Ismailia 41522, Egypt*
[5]*Department of Pharmaceutics, College of Pharmacy, Prince Sattam bin Abdulaziz University, P.O. Box 173, Alkharj 11942, Saudi Arabia*
[6]*Human Anatomy and Embryology Department, Faculty of Medicine, Tanta University Tanta 31527, Egypt*
[7]*Department of Natural Products and Alternative Medicine, Faculty of Pharmacy University of TabuK, Tabuk, Saudi Arabia*
[8]*Department of Pharmaceutics, Faculty of Pharmacy, University of Khartoum, Khartoum, Sudan*

Unedited

Abstract: Ulcerative colitis (UC) is an inflammatory condition of the intestine, resulting from an increase in oxidative stress and pro-inflammatory mediators. In this study, the extract of endophytic bacteria *Rhizobium aegyptiacum* was prepared for the first time using liquid chromatography-mass spectroscopy. In addition, also for the first time, the protective potential of *R. aegyptiacum* was revealed using an in vivo rat model of UC. The animals were grouped into four categories: normal control (group I), *R. aegyptiacum* (group II), acetic acid (AA)-induced UC (group III), and *R. aegyptiacum*-treated AA-induced UC. In group IV, *R. aegyptiacum* was administered at 0.2 mg/kg daily for one week before and two weeks after the induction of UC. After sacrificing the rats on the last day of the experiment, colon tissues were collected and subjected to histological, immunohistochemical and biochemical investigations. There was a remarkable improvement in the histological findings of the colon tissues in group IV, as revealed by hematoxylin and eosin staining, Masson's trichrome staining, and Periodic acid-Schiff staining. Normal mucosal surfaces covered with a straight, intact and thin brush border were revealed. Goblet cells appeared magenta in color, and there was a significant decrease in the distribution of collagen fibers in the mucosa and submucosal connective tissues. All these findings were comparable to the respective characteristics of the control group. Regarding cyclooxygenase-2 immunostaining, a weak immune reaction was shown in most cells. Moreover, the colon tissues were examined using a scanning electron microscope, which confirmed the results of histological assessment. A regular polygonal unit pattern was seen with crypt orifices of different sizes and numerous goblet cells. Furthermore, the levels of catalase (CAT), myeloperoxidase (MPO), nitric oxide (NO), interleukin-6 (IL-6), and interlukin-1β (IL-1β) were determined in the colonic tissues of the different groups using colorimetric and ELISA assays. In comparison with group III, group IV exhibited a significant rise ($p < 0.05$) in CAT level but a substantial decline ($p < 0.05$) in NO, MPO and inflammatory cytokine levels (IL-6 and IL-1β). Based on qRT-PCR, the tumor necrosis factor-alpha gene expression was upregulated in group III, which was significantly downregulated ($p < 0.05$) by treatment with *R. aegyptiacum* in group IV. On the contrary, the heme oxygenase-1 gene was substantially upregulated in group IV. Our findings imply that the oral consumption of *R. aegyptiacum* ameliorates AA-induced UC in rats by restoring and reestablishing the mucosal integrity, in addition to its anti-oxidant and anti-inflammatory effects. Accordingly, *R. aegyptiacum* is potentially effective and beneficial in human UC therapy, which needs to be further investigated in future work.

Key words: Inflammatory bowel syndrome; LC-MS/MS; SEM; Histology; Immunohistochemistry; qRT-PCR

✉ Engy ELEKHNAWY, engy.ali@pham.tanta.edu.eg
Walaa A. NEGM, walaa.egm@pham.tanta.edu.eg
* The two authors contributed equally to this work
Engy ELEKHNAWY, http://orcid.org/0000-0001-8287-1026
Walaa A. NEGM, http://orcid.org/0000-0003-0463-8047

Received Oct. 27, 2023; Revision accepted Feb. 20, 2024;
Crosschecked xxx. xx, 20xx; Published online xxx. xx, 20xx

© Zhejiang University Press 2024

1 Introduction

Most young adults without a gender preponderance suffer from ulcerative colitis (UC), a chronic, inflammatory illness with no known etiology. The prevalence of UC is increasing globally and is greater in industrialized countries (Ben-Horin *et al*., 2022). The definitive feature of UC is mucosal inflammation that begins in the rectum and spreads to the proximal portions of the colon. Clinically, UC typically manifests as persistent and bloody diarrhea. About a third of individuals experience extraintestinal symptoms, such as peripheral arthritis, primary sclerosing cholangitis, and pyoderma gangrenosum (Vavricka *et al*., 2011; Dignass *et al*., 2012).

Inflammation is central to the progress of various complex ailments like autoimmune illnesses and metabolic syndromes, with prostaglandins playing a major regulatory role. Cyclooxygenases such as COX-2 mediate inflammation via catalyzing arachidonic acid metabolism and in turn synthesizing prostaglandins (Le Loupp *et al*., 2015).

Furthermore, when inducible nitric oxide synthase (iNOS) is activated, free radicals are triggered, which hinders the anti-oxidative system and thus could augment the damage to the intestinal mucosa (Wang and DuBois 2010; Piechota-Polanczyk and Fichna, 2014). In addition, the excessive production of reactive oxygen species (ROS) could have a negative impact on the mucosal defense system (Checa and Aran, 2020).

The extended release of pro-inflammatory cytokines, like tumor necrosis factor-alpha (TNF-α), interleukin-6 (IL-6), and interleukin-1β (IL-1β), could trigger apoptosis, which possesses a central role in inflammatory bowel diseases (IBD) like UC. It has been documented that apoptosis is integral to the pathophysiology of IBD (Gautam *et al*., 2013; Liu *et al*., 2022). This is attributed to the induction of apoptosis by the inflammatory process, which alters the function of the mucosal barrier and disturbs gut integrity (Raish *et al*., 2021).

The histological analysis of biopsy samples is essential for making a definite diagnosis, estimating the level of disease activity, assessing the likelihood of healing, and assessing the risk of relapse. Besides, histology is crucial for determining the treatment efficacy and identifying the side effects of treatment and longstanding UC, such as dysplasia (Adamina *et al*., 2021).

The current anti-inflammatory therapeutics for UC treatment suffer from many side effects like diarrhea, allergic responses, lymphopenia, vomiting, and elevation of the liver enzyme levels (Bruscoli *et al*., 2021). Therefore, it is critical to find novel therapeutics that could hinder the inflammatory cascade associated with the pathological consequences of UC.

Endophytic bacteria have the potential to both enhance the growth and yield of plants and serve as biocontrol agents (Rana *et al*., 2020). They respond to biotic and abiotic hazards by enhancing biological N2-fixation, producing phytohormones soluble phosphate, inhibiting ethylene (C_2H_2) biosynthesis, and exhibiting bio-control action (Singh *et al*., 2017). Additionally, they can control the synthesis of secondary metabolites with significant therapeutic effects and exert a variety of biological effects (Twaij and Hasan, 2022).

Natural compounds represent a vital source for many bioactive therapeutics toward different ailments. Many researchers have investigated the potential therapeutic benefits of various plant and microbe metabolites against UC (Fan *et al*., 2020; Xue *et al*., 2023; Khare *et al*., 2020). To our knowledge, it is the first time that the endophytic bacteria *Rhizobium aegyptiacum* has been chemically analyzed using LC/MS, and its therapeutic potential on UC has been investigated in an animal model.

2 Materials and methods

2.1 Chemicals and drugs

All chemicals and solvents used were obtained from Sigma (USA), and culture media were obtained from Oxoid, UK.

unedited

2.2 Isolation of *R. aegyptiacum* endophytic bacteria

Healthy leaves of Acalypha hispida Burm. f. were harvested in summer from the plantation of the Faculty of Pharmacy, Tanta University, Egypt. The plant material was identified by Dr. Esraa Ammar, Faculty of Science, Tanta University. After rinsing, the surface of Acalypha leaves was sterilized with 70% ethyl alcohol for two minutes until drying. Subsequently, they were cut aseptically into small sections and imprinted onto yeast extract mannitol agar (YEMA) with incubation for 72 h at 28℃ in the dark. Finally, pure strains of *R. aegyptiacum* were obtained.

2.3 Identification of the endophytic bacteria

After the extraction of total DNA from the endophytic bacteria using a DNA extraction kit (Qiagen, Germany), the bacterial universal ribosomal 16S rRNA gene was employed to characterize the isolated strain. The forward and reverse primer was 5-AGAGTTTGATCCTGGCTCAG-3 and 5`-GGTTACCTTGTTACGACTT-3`, respectively (Lane 1991). We determined the amplified gene sequences using ABI PRISM® 3100 Genetic Analyzer (Applied Biosystems, Thermo Fisher Scientific, USA). Finally, the obtained sequences were deposited in Gene Bank (https://blast.ncbi.nlm.nih.gov/Blast.cgi). The sequence homology was detected using the BLAST tool. The phylogenetic tree, was obtained using ClusteralW software analysis (www.ClusteralW.com).

2.4 Cultivation of *R. aegyptiacum*

The culture was prepared by first inoculating the endophytic bacteria *R. aegyptiacum* under sterile conditions into an Erlenmeyer conical flask with cotton plugs, that had been previously autoclaved and contained 500 ml yeast mannitol broth (10 flasks, 1 L each), and then incubating at 28℃ for 72 h in the dark.

2.5 Liquid chromatography-mass spectrometry (supplementary data)

The LC-MS/MS analysis of the prepared endophytic bacteria *R. aegyptiacum* extract was performed according to previously reported methods (Attallah *et al*., 2022a; Elmongy *et al*., 2022).

2.6 Acetic acid (AA)-induced UC experiment

2.6.1 Animals

Forty male albino rats weighing approximately 210 g and aged 8–10 weeks were utilized, which were kept under standard conditions. All procedures performed in this study were accepted by the Medical Research Ethics Committee, Faculty of Medicine, Tanta University (36264PR357/9/23).

2.6.2 Induction of UC (supplementary data)

UC was induced as previously described (Ansari *et al*., 2021).

2.6.3 Experimental design

The rats were allocated into four groups (n=10) as follows:

Group I (control group): The rats received saline by oral gavage for three weeks. They were administered two milliters of saline in a single dose into the colon through a rubber catheter on the seventh day.

Group II (*R. aegyptiacum* group): Over the course of three weeks, the rats were given *R. aegypticaum* by oral gavage at a dosage of 0.2 mg/kg solution dissolved in carboxymethyl cellulose.

unedited

Group III (AA-induced UC group): same as the untreated group but with AA-induced colitis.

Group IV (*R. aegyptiacum*-treated AA-induced UC group): AA-induced colitis with the concomitant administration of *R. aegyptiacum* by oral gavage at 0.2 mg/kg daily for one week before and 2 weeks after the induction of colitis.

2.6.4 Histological and immunohistochemical analysis

Distal colon samples from all studied groups were embedded in paraffin blocks after fixation in formalin. A routine histological examination of 5–6 μm thick slices was performed by staining with hematoxylin and eosin (Bancroft and Gamble, 2008). Periodic acid-Schiff (PAS) reagent was used to detect goblet cells and the brush border of surface epithelium, and Masson Trichrome Stain was employed to detect the collagen fibers of connective tissue (Hsiao *et al*., 2021; Alherz *et al*., 2022). A morphometric analysis of mean number of goblet cells and the mean area percentage of collagen fibers was conducted by using ten non-overlapping readings obtained for each slide in all groups via image analysis tools (Image J). For immunohistochemical analysis, the colonic sections were deparaffinized, rehydrated, and incubated overnight at 4℃ with rabbit monoclonal COX-2antibody (EPR12012, 1/250, ab179800, Abcam).

2.6.5 Scanning electron microscopy (SEM) (supplementary data)

2.6.6 Colorimetric evaluation of catalase (CAT), myeloperoxidase (MPO) and nitric oxide (NO) in colon tissues

The CAT, MPO and NO levels were evaluated in colon homogenates by CAT, MPO and NO assay kits (Abcam, USA).

2.6.7 Detection of IL-6 and IL-1β levels using ELISA

The IL-6 and IL-10 levels were determined in the colon tissue homogenates using ELISA kits (Sun Red Biotechnology Co., China) and an ELISA microplate reader at 450 nm.

2.6.8 qRT-PCR for TNF-α and heme oxygenase-1 (HO-1)

After the extraction of total RNA by TRIzols (Life Technologies, USA) (Livak and Schmittgen, 2001), it was converted to cDNA by the QuantiTect kit (Qiagen, USA). Then, cDNA was amplified by the Maxima SYBR Green Master Mix (Thermo Fisher Scientific, USA). The employed primers are documented in Table S1 (Mi *et al*., 2017).

2.7 Statistical analysis

ANOVA was performed to detect significant differences among the studied groups. The results were expressed as mean ± standard deviation (SD) using Graph Pad Prism software (USA), and the statistical significance was determined at $p < 0.05$.

3 Results

3.1 Identification of the isolated endophytic bacteria

The bacterial isolate was identified as *Rhizobium aegyptiacum* as confirmed in Table 1 and Fig. S1.

unedited

Table 1 Identification data of *R. aegyptiacum* by 16S rRNA sequencing

Accession number	Identification	Highly similarity Isolates	Highly similarity isolates Accession number	Identity %
ON100826	*Rhizobium aegyptiacum strain*	*Rhizobium aegyptiacum strain 1010 16S ribosomal RNA, partial sequence*	NR_137399.1	99.93

3.2 Phytochemical profiling

A total of 31 compounds were tentatively identified in the *R. aegyptiacum* extract by using both the positive and negative modes of LC-ESI-MS/MS. The main components were several types of amino acids, flavonoids, coumarins, and other glycosylated compounds. The obtained metabolite profile is presented in Table 2 and Fig. S2 and S3. The mass/mass spectra shown in Fig. 1 and 2 display the fragmentation pattern of the most abundant detected metabolites in positive and negative modes.

Table 2. Phytochemical profiling of *R. aegyptiacum* extract using LC-ESI-MS/MS different modes

No.	Rt (min)	Precursor *m/z*	Error ppm	Name	Formula	Adduct ion	MS/MS spectrum	Class
1	0.97	191.0201	-0.6	Citric acid	$C_6H_8O_7$	$[M-H]^-$	173.0089, 129.0194, 87.0089, 57.0347	Tricarboxylic acids and derivatives
2	1.05	117.0185	0	Succinic acid	$C_4H_6O_4$	$[M-H]^-$	117.0191, 99.0074, 73.0296, 55.0187	Dicarboxylic acids and derivatives
3	1.05	161.0441	-2.5	3-Hydroxy-3-Methylglutaric acid	$C_6H_{10}O_5$	$[M-H]^-$	101.213, 99.0452, 59.0151, 57.0341	Hydroxy fatty acids
4	1.07	133.0136	-0.9	Malic acid	$C_4H_6O_5$	$[M-H]^-$	115.0042, 89.0272, 87.0099, 72.9937, 71.0143	Beta hydroxy acids and derivatives
5	1.15	104.1069	-5.4	Choline	$C_5H_{14}NO$	$[M]^+$	60.0814, 58.0657	Cholines
6	1.16	195.052	0.8	Gluconic acid	$C_6H_{12}O_7$	$[M-H]^-$	177.0394, 160.8413, 75.0089, 59.0141	Medium-chain hydroxy acids and derivatives
7	1.17	162.1123	-0.7	Carnitine	$C_7H_{15}NO_3$	$[M+H]^+$	103.0386, 102.0902, 85.0284, 60.0805	Carnitines
8	1.20	144.0685	0.6	4-acetamidobutanoic acid	$C_6H_{11}NO_3$	$[M-H]^-$	102.0563, 100.0782, 58.0302, 54.0352	Gamma amino acids and derivatives
9	1.25	175.0582	-0.8	L-Arginine	$C_6H_{14}N_4O_2$	$[M+H]^+$	158.0902,	L-alpha-amino

unedited

							116.0687, 70.0648, 60.0542	acids
10	1.25	146.1192	0.9	Deoxycarnitine	$C_7H_{15}NO_2$	$[M+H]^+$	87.0442, 60.0820, 58.0663	Straight chain fatty acids
11	1.27	118.0866	-2.3	Glycine-Betaine	$C_5H_{11}NO_2$	$[M+H]^+$	59.0642, 58.0723	Alpha amino acids
12	1.29	181.0722	0.1	Mannitol	$C_6H_{14}O_6$	$[M-H]^-$	163.0617, 101.0243, 89.0245, 59.0142	Sugar alcohols
13	1.32	341.1127	0.9	Palatinose	$C_{12}H_{22}O_{11}$	$[M-H]^-$	222.0667, 179.0563, 119.0351, 89.0242	*O*-glycosyl compounds
14	1.76	130.0497	0.3	L-5-Oxoproline	$C_5H_7NO_3$	$[M+H]^+$	84.0439, 56.0491	Alpha amino acids and derivatives
15	2.04	164.0707	0.3	Phenylalanine	$C_9H_{11}NO_2$	$[M-H]^-$	147.0457, 103.0561, 91.0566, 72.0093	Phenylalanine and derivatives
16	2.10	162.078	0.8	*O*-Acetyl-L-homoserine	$C_6H_{11}NO_4$	$[M+H]^+$	127.0396, 120.0660, 102.0553	L-alpha-amino acids
17	2.15	166.0863	0	Phenylalanine	$C_9H_{11}NO_2$	$[M+H]^+$	120.0809, 103.0567, 77.0380	Phenylalanine and derivatives
18	6.03	211.1445	-0.4	3-butan-2-yl-2,3,6,7,8,8a-hexahydropyrrolo[1,2-a]pyrazine-1,4-dione	$C_{11}H_{18}N_2O_2$	$[M+H]^+$	183.1529, 154.0747, 138.1287, 70.0645	Alpha amino acids and derivatives
19	6.75	209.081	0.7	3,4-Dimethoxy cinnamic acid	$C_{11}H_{12}O_4$	$[M+H]^+$	191.0711, 165.0715, 135.0810, 107.0856	Coumaric acids and derivatives
20	8.43	285.0393	0.4	Luteolin	$C_{15}H_{10}O_6$	$[M-H]^-$	268.0384, 257.0463, 241.0507	Flavones
21	8.60	227.0912	0.8	2-Hydroxyjasmonic acid	$C_{12}H_{18}O_4$	$[M+H]^+$	191.0674, 149.0944, 131.0860, 107.0820	Jasmonic acids
22	8.76	254.1394	0.2	N-[1-(4-methoxy-6-oxopyran-2-yl)-2-methylbutyl] acetamide	$C_{13}H_{19}NO_4$	$[M+H]^+$	212.1278, 156.0659, 125.0234	Pyranones and derivatives
23	8.82	245.1367	-0.9	8-hydroxy-3-methoxycarbonyl-2-methylidenenonanoic acid	$C_{12}H_{20}O_5$	$[M+H]^+$	177.0915, 149.0961, 131.0852, 79.0540	Medium-chain hydroxy acids and derivatives
24	9.21	434.1786	-0.6	(3Z)-6-Hydroxy-3-(1H-imidazol-5-ylmethylene)-12-methoxy-7a-(2-methyl-3-	$C_{23}H_{23}N_5O_4$	$[M+H]^+$	403.1638, 334.0912, 289.0704,	Pyridoindolones

unedited

				buten-2-yl)-7a,12-dihydro-1H,5H-imidazo [1',2':1,2] pyrido[2,3-b] indole-2,5(3H)-dione			261.0754	
25	9.52	299.0548	0.9	kaempferide	$C_{16}H_{12}O_6$	$[M-H]^-$	284.0270, 255.0664, 151,0023	Flavonols
26	9.80	237.0789	-0.5	5,6,7-trimethoxychromen-2-one	$C_{12}H_{12}O_5$	$[M+H]^+$	222.0513, 207.0274, 179.0326	Coumarins and derivatives
27	12.59	432.1649	0	(3Z)-6-Hydroxy-3-(1H-imidazol-5-ylmethylene)-12-methoxy-7a-(2-methyl-3-buten-2-yl)-7a,12-dihydro-1H,5H-imidazo[1',2':1,2]pyrido[2,3-b]indole-2,5(3H)-dione	$C_{23}H_{23}N_5O_4$	$[M-H]^-$	332.0771, 304.0831, 276.0894, 177.0417	Pyridoindolones
28	13.18	343.2918	-0.4	Cocamidoprpyl Betaine	$C_{19}H_{38}N_2O_3$	$[M+H]^+$	240.2325, 183.1727, 57.0690	Alpha amino acids
29	16.26	639.1719	-0.9	Secalonic acid	$C_{32}H_{30}O_{14}$	$[M+H]^+$	621.1589, 589.1319, 579.1508, 561.1398	Xanthones
30	18.09	277.2157	-1	Linolenic acid	$C_{18}H_{30}O_2$	$[M-H]^-$	233.1540, 208.9221	Lineolic acids and derivatives
31	23.22	281.2488	0.8	Elaidic acid	$C_{18}H_{34}O_2$	$[M-H]^-$	281.2472, 263.2372	Long-chain fatty acids

unedited

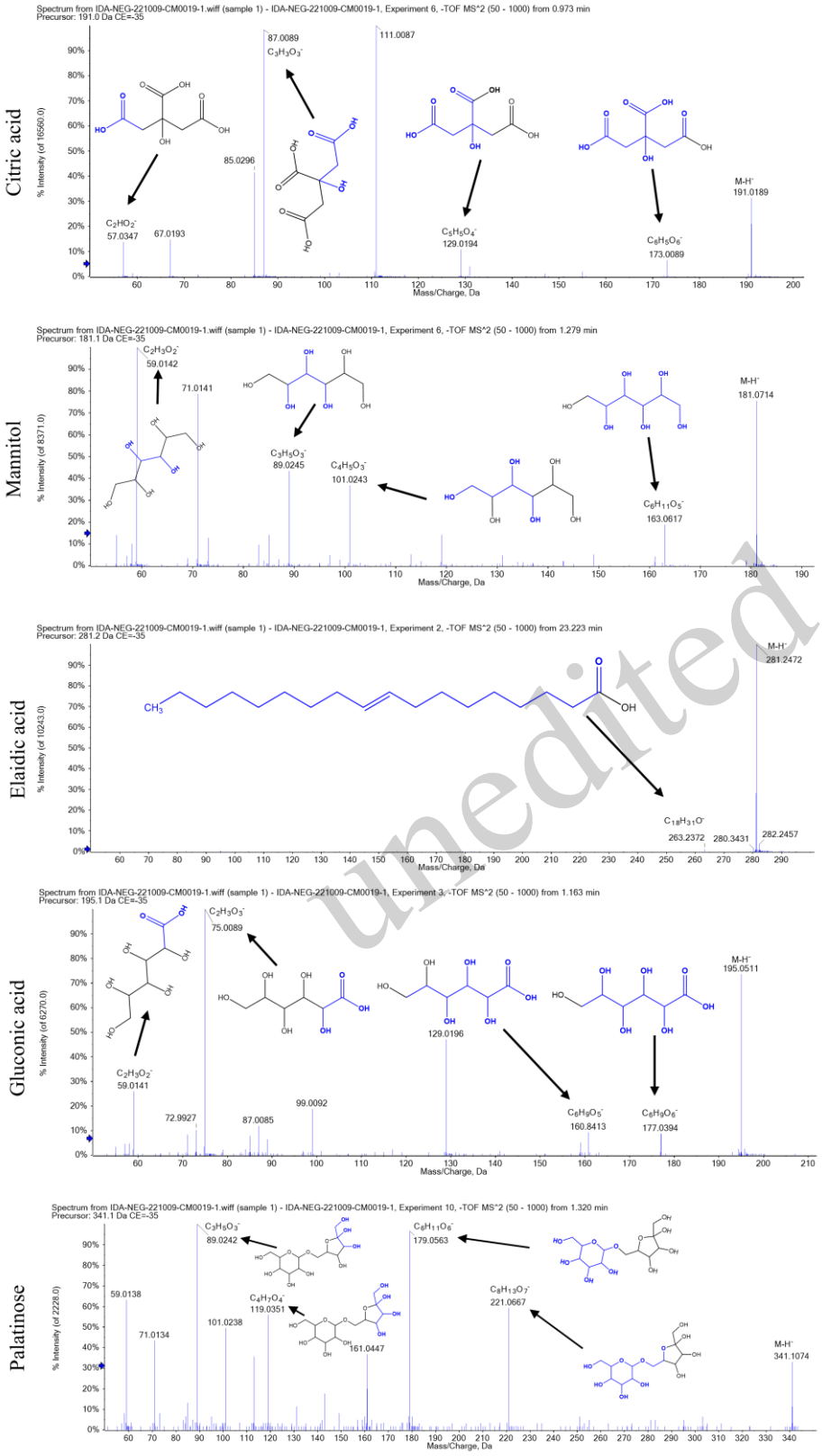

unedited

Fig. 1 The most abundant detected compound in negative LC-MS mode

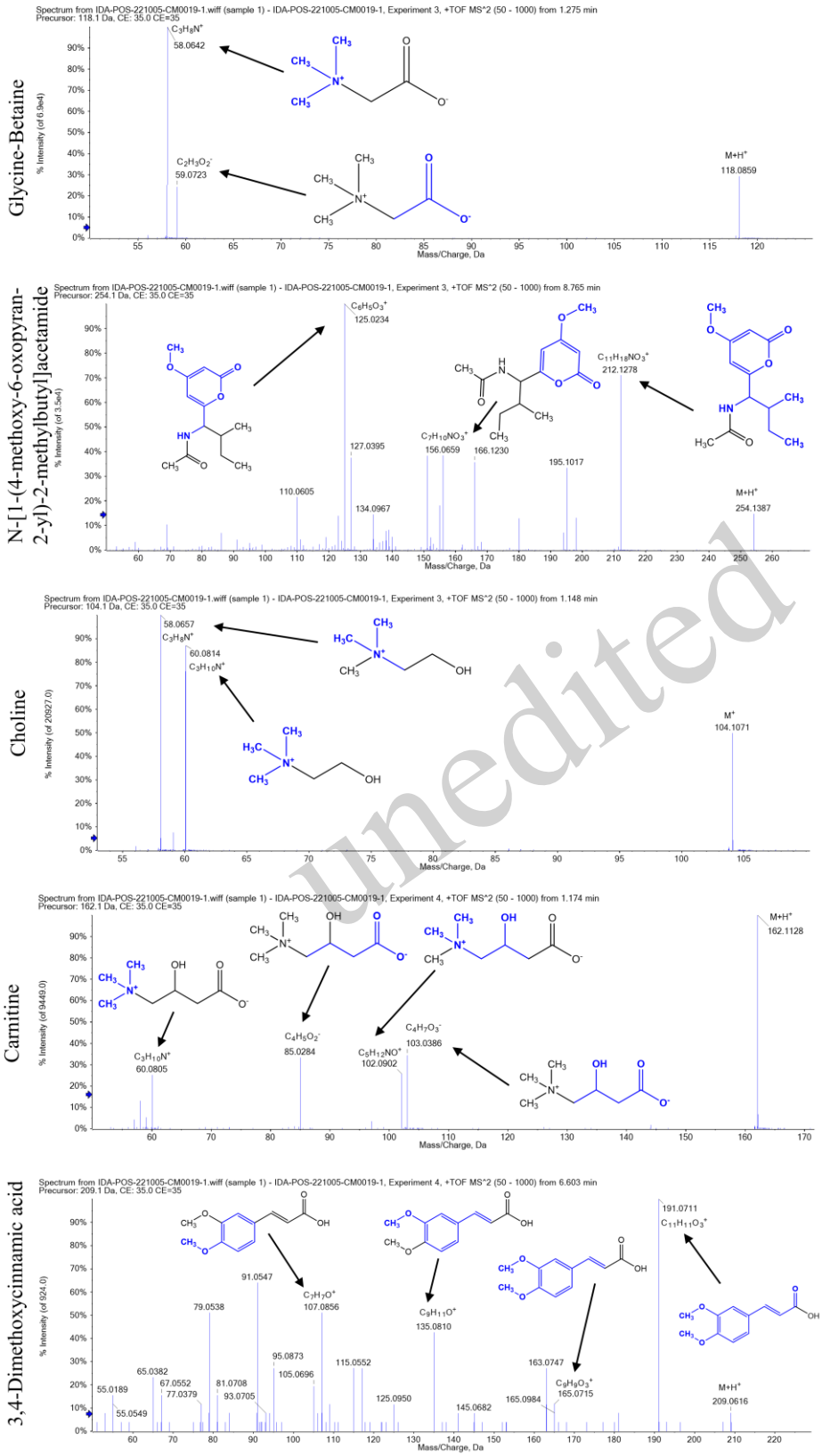

unedited

Fig. 2 The most abundant detected compound in positive LC-MS mode

3.3 H&E staining

The H&E-stained colonic tissues of groups I and II revealed a normal mucosal surface covered with a thin striated brush border. The mucosal lamina propria (LP) contained simple tubular intestinal glands (crypts of Lieberkühn). The crypts were long, deep and straight, and lined with numerous goblet cells. Mononuclear cells could be observed to fill the space between glands in the lamina propria (Fig. 3, a-d). On the other hand, in group III with A-A induced colitis, structural changes of the mucosa and epithelial abnormalities were revealed, including focal loss of surface epithelium and part of the lamina propria with widespread architectural crypt distortion and increased cellularity of the lamina propria in the form of disseminated inflammatory cellular infiltration in the glandular tissue (Fig. 3, e, f). Also, there was an apparent reduction in the number of goblet cells with crypt cysts and abscess formation. Meanwhile, the concomitant administration of *R. aegyptiacum* with AA in group IV revealed a histological image resembling that of control groups. However, there was focal inflammatory cellular infiltration and widening of the submucosa (Fig. 3, g, h).

unedited

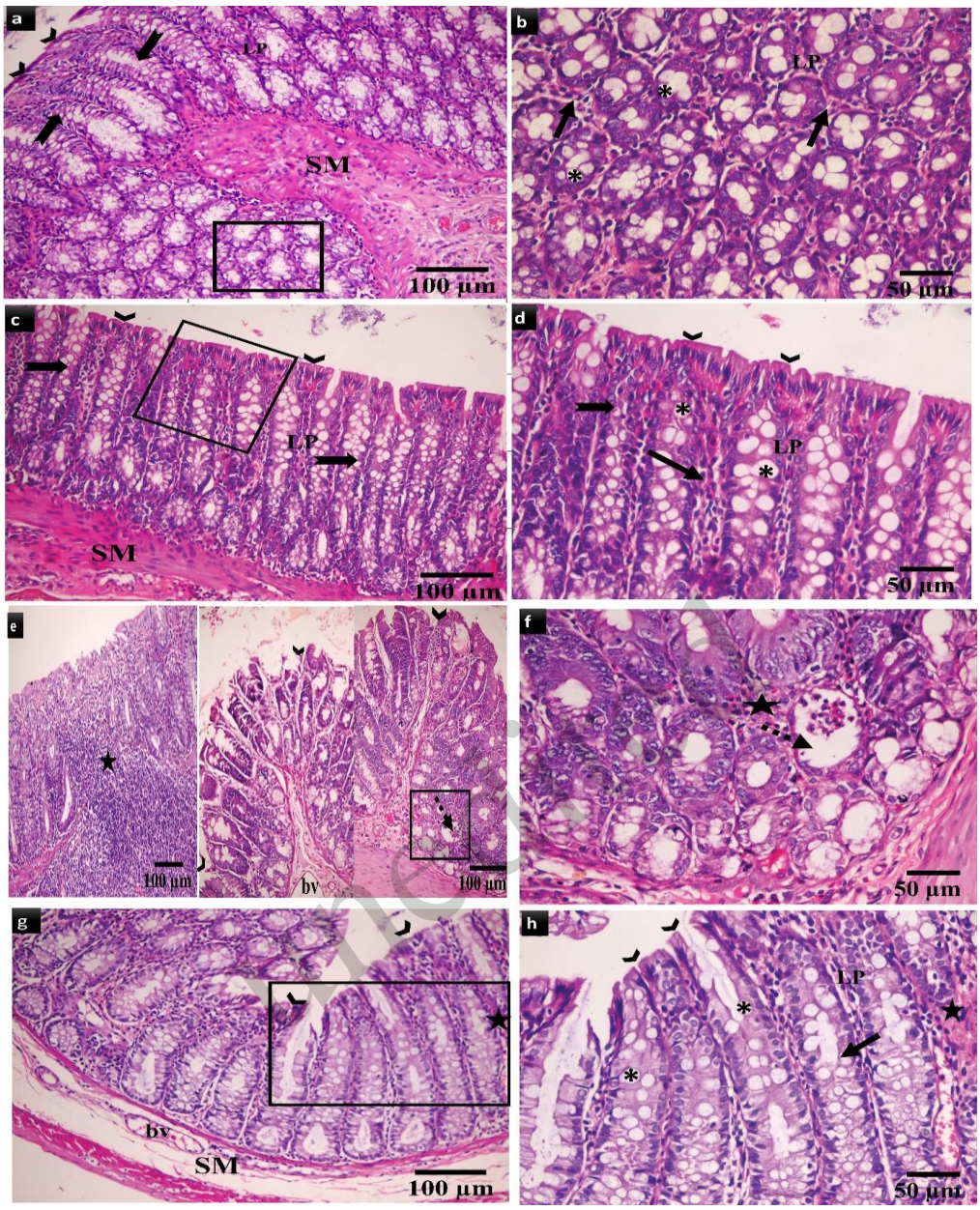

Fig. 3 Light microscope images of the distal colon sections of adult male albino rats in all studied groups. Note: the images b, d, f, and h represent higher magnifications of selected square areas of images a, c, e, and g, respectively. (a-d) Group I & II show normal colonic mucosa and submucosa (SM). The mucosal surface is covered with a thin striated brush border (arrowheads). The mucosal lamina propria (LP) contains simple tubular intestinal glands (crypts of Lieberkühn). The crypts are long, deep and straight (Bifid arrows), and are lined by numerous goblet cells (asterix). Mononuclear cells fill the space between glands in the lamina propria (arrows). (e,f) Group III with A-A induced colitis, showing focal loss of surface epithelium and part of the lamina propria (arrowheads) with inflammatory cellular infiltration in the glandular tissue (star). Furthermore, there is an apparent reduction in the number of goblet cells and crypt cyst formation (dashed arrow). (g, h) Group IV shows a normal histological image of the colonic mucosa with a straight intact brush border (arrow heads) and numerous goblet cells in the glandular tissue (asterisk). However, focal inflammatory cell infiltration (stars) and widening of the submucosa (SM) exist. (H&E × 200, scale bar = 100 µm, H&E × 400, scale bar = 50 µm).

3.4Staining with PAS reagent

The analysis of PAS-stained colonic sections of both groups I and II exhibited intact PAS-positive thin brush borders of columnar cells. In contrast, goblet cells were detected in the epithelium with the characteristic magenta color of mucin secretion (Fig. 4, a, b). Meanwhile, group III showed an evident statistically significant reduction in goblet cells and an interrupted brush border (Fig. 4, c). On the other hand, group IV exhibited a straight, intact, thin brush border, and goblet cells appeared magenta in color without statistically significant differences compared to control group I (Fig. 4, d).

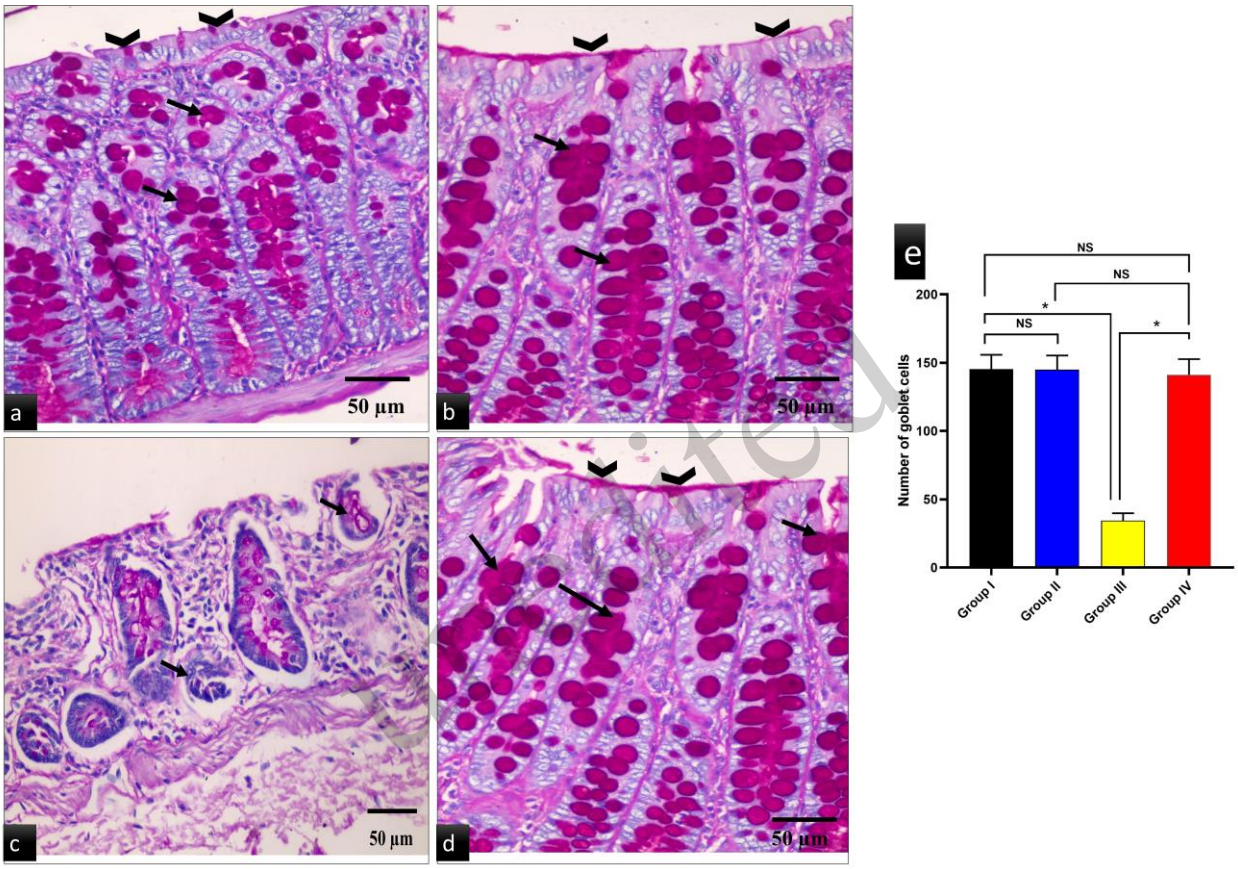

Fig. 4 Sections of the distal colon of adult male albino rats in all studied groups. (a–d) PAS (Periodic acid-Schiff) stained sections. (a, b) Control and rhizobium groups showing a PAS-positive thin brush border (arrowheads) and goblet cells colored magenta (arrows). (c) A.A. group presenting a reduction in the number of goblet cells (arrows) with the interruption of the brush border. (d) Rhizobium + A.A. group showing a thin brush border without interruption (arrowheads) and goblet cells (arrows) positively stained with magenta-coloured mucin secreted from the cells. (e) Number of goblet cells in all studied groups. The data are expressed as mean ± SD. NS means no significant difference, and the single asterisk represents significant difference (p < 0.05) where n=10. (PAS = 400, scale bar = 50 m).

3.5 Masson's trichrome staining

The examination of Masson's-stained colonic sections of both groups I and II revealed the arrangement and distribution of collagen fibers in the lamina propria between the tubular glands and submucosal connective tissue (Fig. 5, a-d). In contrast, group III exhibited a statistically significant increase in the distribution of collagen fibers in the mucosa and submucosal connective tissue (Fig. 5, e and f). Meanwhile, group IV showed

a statistically significant decrease in the distribution of collagen fibers in the mucosa and submucosal connective tissue in comparison to group II, with no statistically significant difference relative to the control groups (Fig. 5, g and h).

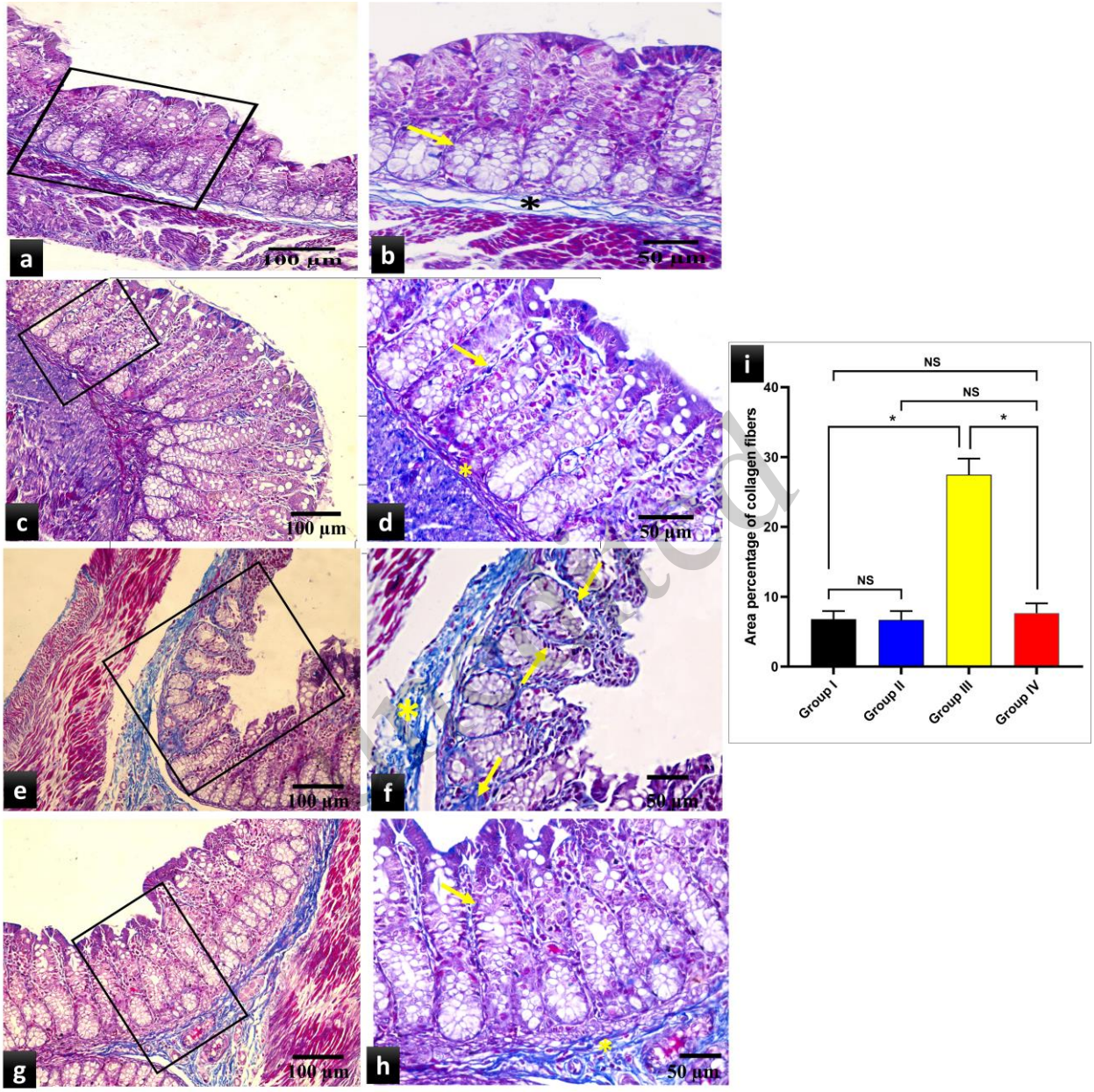

Fig. 5 Sections of the distal colon of adult male albino rats in all studied groups. (a–d) Masson's trichrome-stained sections; collagen fibers in the mucosa (arrows) and in the submucosa (asterisk). Note: the images numbered b, d, f, and h represent higher magnifications of selected square areas of images a, c, e, and g, respectively. (a, b) Control and rhizobium groups showing the arrangement of collagen fibers in the lamina propria between glands and in the submucosal connective tissue, (c) A.A. group showing an evident increase in collagen fibers in the mucosa and submucosal connective tissue; (d) Rhizobium + A.A. group exhibiting some collagen fibers in the mucosa and submucosal connective tissue. (e) Area percentage of collagen fibers in all studied groups. All data are expressed as mean ± SD. NS means no significant difference, and the single asterisk represents significant difference ($p < 0.05$), where n=10. (Masson's trichrome staining × 400, scale bar = 50 µm).

3.6 Immunohistochemical study of COX-2 stained sections

The colonic tissues in group III (AA-induced UC) rats had strong positive COX-2 immunoreactivity, with a statistically significant increase in the area percentage of COX-2 positive immunostaining relative to both groups I and II. At the same time, group IV showed a weak positive reaction without a statistically significant difference compared to the control groups, and a statistically significant decrease in the area percentage of COX-2 positive immunostaining relative to group III (Fig. 6).

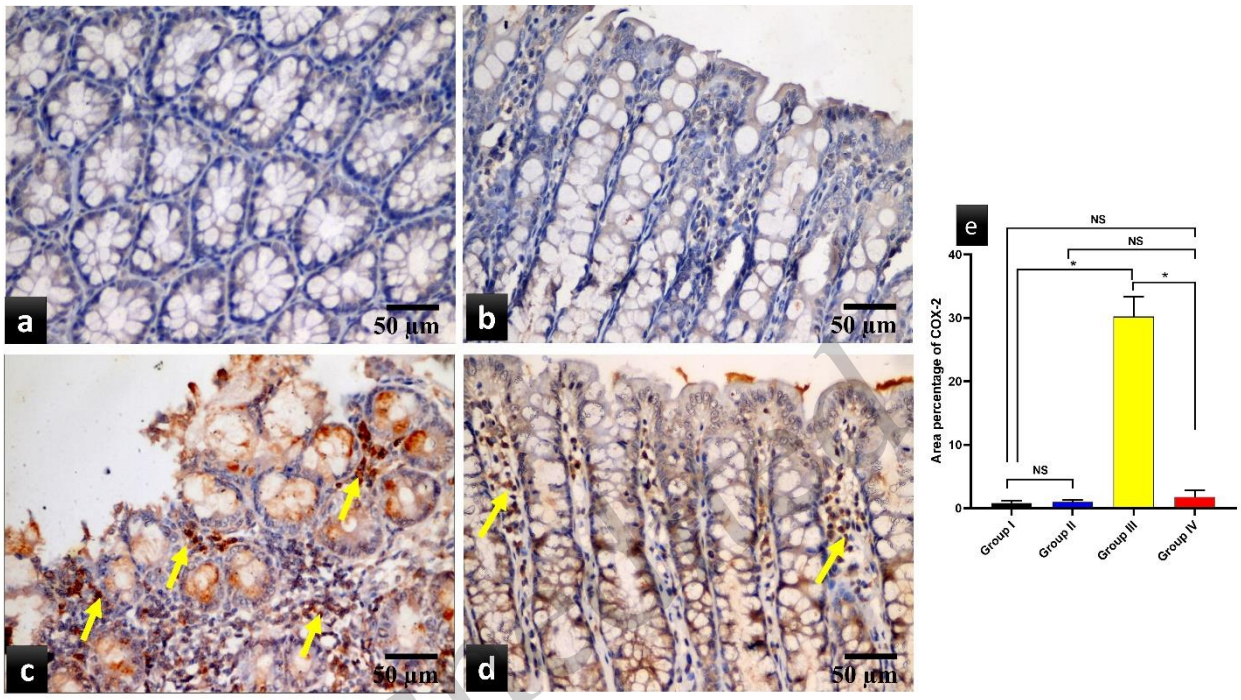

Fig. 6 Sections of the distal colon of adult male albino rats in different studied groups stained by COX-2. (a) Control groups with a negative COX-2 immune reaction in colonic cells. (b) Rhizobium group showing a negative expression of COX-2 immune reaction in all cells. (c) A.A. group presenting a strong positive immune reaction in surface epithelial and glandular cells (yellow arrows). (d) Rhizobium + A.A. with weak immune reaction in most cells (arrows). (e) Area percentage of COX-2 in all studied groups. All data are expressed as mean ± SD. NS means no significant difference, and the single asterisk represents significant difference (p < 0.05), where n=10 (COX-2 immune reaction in the cells immunostaining = 400, scale bar = 50 m).

3.7 SEM

SEM examination of the colonic epithelium of groups I and II revealed a regular pattern of polygonal units with regular size separated by deep gutters. The epithelium invaginated to form many crypts, and numerous goblet cells could be seen (Fig. 7, a-d). Group III samples exhibited enlarged crypt orifices, ulceration of surface epithelium and disorganization of polygonal units. In addition, few goblet cells were recognized (Fig. 7, e, f). Group IV (*R. aegyptiacum* +A. A) demonstrated a regular polygonal unit pattern with crypt orifices of different sizes (c) and numerous goblet cells similar to those of control groups (Fig. 7, g, h).

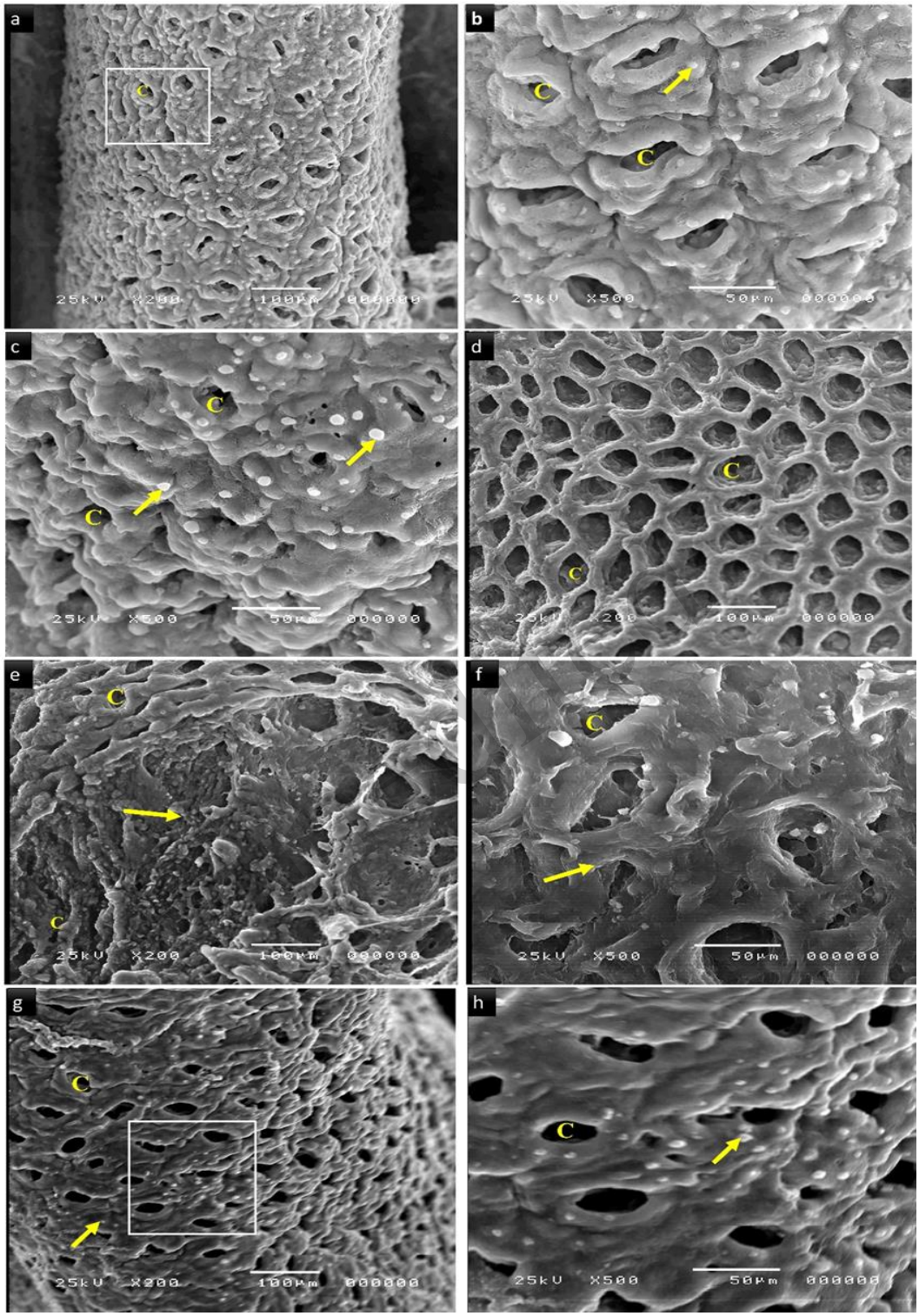

Fig. 7 Representative scanning electron microscopy (SEM) images of the distal colon in all studied groups. (a-c) Groups I and II show a regular pattern of polygonal units with regular size separated by deep gutters; the arrows point to goblet cells and the crypt opening (C). (d-f) A.A. group III showing d, enlarged crypt orifices (c), e, ulceration of surface epithelium (arrows), and disorganization of polygonal units. Few goblet cells are recognized. (g, h) Group IV (*R. aegyptiacum* +A. A) present a regular polygonal unit pattern with crypt orifices of different sizes (c) and numerous goblet cells. (SEM x 200, scale bar = 100 µm; SEM x 500, scale bar = 50 µm).

3.8 Colorimetric studies

In group IV, a significant rise ($p < 0.05$) in CAT level was revealed in comparison with group II. On the other hand, group IV showed a substantial decline ($p < 0.05$) in NO and MPO levels (Fig. 8).

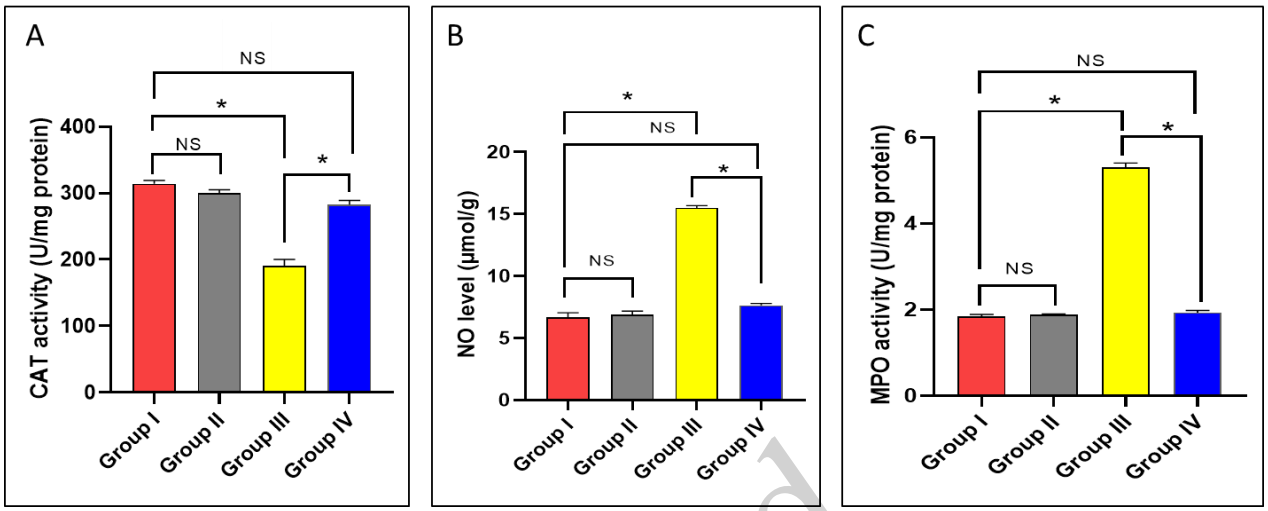

Fig. 8 Charts presenting the levels of: a) CAT, b) NO, and c) MPO in the different experimental groups. NS designates no significant difference ($p < 0.05$), and the asterisk designates significant difference ($p < 0.05$), where n=10.

unedited

3.9 ELISA analyses

Group IV samples presented a substantial decline ($p < 0.05$) in the levels of inflammatory cytokines IL-6 and IL-1β in comparison with group III (Fig. 9).

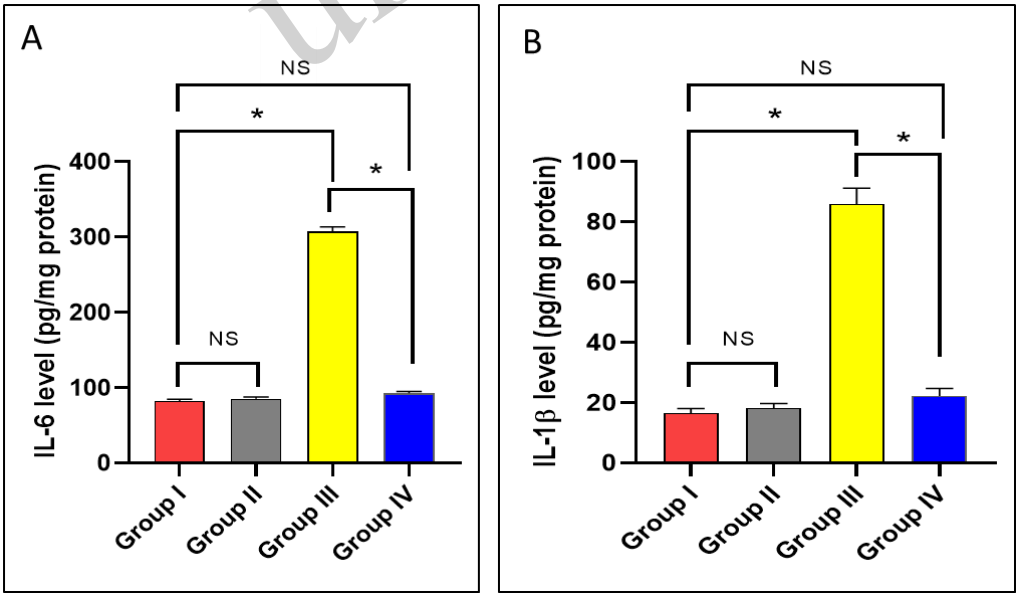

Fig. 9 The levels of a) IL-6 and b) IL-1β in the studied groups. NS designates no significant difference ($p < 0.05$). The asterisk designates significant difference ($p < 0.05$), where n=10.

3.10 qRT-PCR studies

We observed an upregulation of the TNF-α gene expression in group III, which was significantly downregulated ($p < 0.05$) by treatment with *R. aegyptiacum* in group IV. On the other hand, a substantial upregulation of the HO-1 gene was revealed in group IV (Fig. 10).

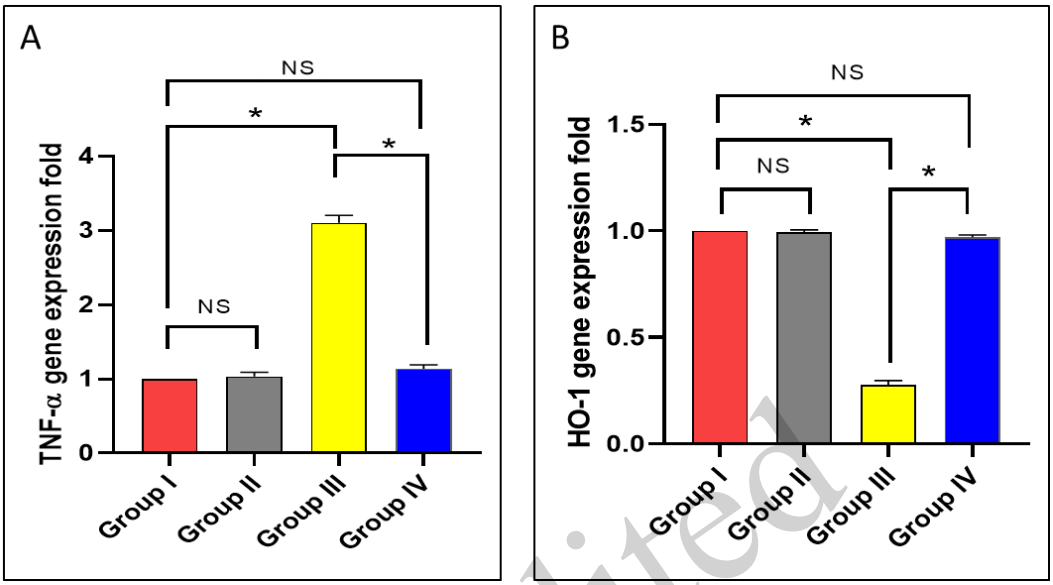

Fig. 10 Fold change in a) TNF-α and b) HO-1 gene expression in different groups. NS designates no significant difference ($p < 0.05$). The asterisk designates significant difference ($p < 0.05$), where n=10.

unedited

4 Discussion

Plants can have associations with different members of the ecosystem living in the surrounding environment (Almukainzi *et al*., 2022). Microorganisms, especially bacteria, are vital for their beneficial associations with various plants (Abdelaziz *et al*., 2019). These bacteria form mutualistic interactions with several advantages to their host. One of these is assisting plants in withstanding different types of stresses that could hinder their growth (Elekhnawy and Negm, 2022). Several bioactive metabolites with pharmacological activities have been isolated from medicinal plant endophytes and structurally identified using various conventional and modern methods. These metabolites have given researchers a starting point to build upon as they continue to create and formulate bioactive molecules into effective medicines with wide-ranging applications in the health care system and many other facets of human existence (Quettier *et al*., 2000; Attallah *et al*., 2022b). Endophytes are typically connected to the secondary metabolites and therapeutic properties of medicinal plants (Strobel and Daisy, 2003). To this end, the current study isolated an endophytic bacterial isolate from *A. hispida* leaves and identified it using 16S rRNA sequencing. Then, LC-MS/MS was performed to determine the bioactive components of the endophytic bacteria. The identified metabolites were found to belong to several phytochemical classes, including amino acids, flavonoids, coumarins, and other glycosylated compounds. The major detected metabolites in the negative mode were citric acid, elaidic acid, mannitol, gluconic acid, and palatinose, while those in the positive mode included glycine-betaine, N-[1-(4-methoxy-6-oxopyran-2-yl)-2-methylbutyl] acetamide, choline, carnitine, and 3,4-dimethoxy cinnamic acid.

The protective potential of the endophytic *R. aegyptiacum* against the AA-induced UC in rats was

investigated for the first time. In the present study, assessment with H&E staining revealed that, in the AA-induced colitis group, structural changes of mucosa and epithelial abnormalities were present, including focal loss of surface epithelium and disseminated inflammatory cellular infiltration, which were in accordance with a previous study (Bertevello *et al*., 2005). Ansari et al. (Ansari *et al*., 2022) indicated that the AA-induced colitis group stained with PAS displayed deceptively decreased goblet cells and reduced mucin score, also reported in the current study. The mucosal structure damage, inflammation, and reduction in goblet cells numbers were enhanced by the administration of *R. aegyptiacum*. COX-2 was expressed in mucosal epithelial cells in the AA-induced colitis group and this expression was significantly decreased by the administration of *R. aegyptiacum*. Endophytic metabolites had been suggested as a possible source of recent natural antioxidants. Liu et al. (Liu *et al*., 2007) reported that the endophytic fungus Xylaria sp. obtained from the leaves of ginkgo biloba exhibited antioxidant activity (Khairy *et al*., 2018).

The main pathophysiology of UC includes increase in oxidative stress and pro-inflammatory mediators like TNF-α, IL-6 and IL-1β. This was confirmed in the AA-induced UC group in the current study, in line with previous investigations (Raish *et al*., 2021; Shahid *et al*., 2022; Li *et al*., 2020; Ran *et al*., 2008). COX-2 produces PGE2, which in turn triggers intestinal edema and hyperemia (Abdallah *et al*., 2020; Alotaibi *et al*., 2022). Thus, the increase in COX-2, as revealed by the immunohistochemical investigations, along with the substantial increase in the MPO and NO, have resulted in augmentation of the inflammatory process and depletion of the anti-oxidative system (represented by CAT activity) in the colon tissues (Khairy *et al*., 2018). The administration of *R. aegyptiacum* markedly ameliorated all such pathological changes. Interestingly, certain identified compounds in the *R. aegyptiacum* extract had been documented to have anti-inflammatory and/or antioxidant potential; different studies have demonstrated the anti-inflammatory potential of the compounds of the bacterial extract. Peyrottes et al. (Peyrottes *et al*., 2022) reported that O-acetyl-L- decreased the IL-6 level in murine macrophage cell lines stimulated with lipopolysaccharide (LPS) and interferon-γ (IFN-γ). Wang *et al*. (Wang *et al*., 2021) documented that leucine-proline-phenylalanine-derived peptide suppressed the mRNA expression of inducible nitric oxide synthase (iNOS), COX-2, and TNF-α in LPS-irritated RAW264.7. In addition, Aziz *et al*. (Aziz *et al*., 2018) proved luteolin's strong *in vivo* and *in vitro* anti-inflammatory activity. The action mechanism of luteolin includes the NF-κB pathway, mitogen-activated protein kinases (MAPK) pathway, and the signal transducer and activator of transcription 3 (STAT3) pathway.

Many previous studies have reported the beneficial impacts of other groups of bacteria (probiotics) in treating UC (Blacher *et al*., 2017; Popov *et al*., 2021). Probiotics like Bifidobacterium and Lactobacillus can improve intestinal barrier integrity, which is attained by metabolizing short-chain fatty acids, tryptophan and other chemicals, leading to the increased production of mucin and tight junction proteins in the intestinal epithelial cells (Lavelle *et al*., 2020; Kaur *et al*., 2020). Further evidence suggests the ability of probiotics to regulate intestinal immunity, preventing the excessive activation of the intestinal immune cells and reducing the levels of certain pro-inflammatory mediators, such as IL-6, TNF-α, and IL-1β. Moreover, it was proved that probiotics could increase the levels of anti-inflammatory factors, like IL-10 and transforming growth factor beta (TGF-β). This, along with inhibited expression of the nuclear factor kappa-beta (NF-κB) signaling pathway, could improve intestinal inflammation (Lavelle *et al*., 2020). Overall, this study provides a basis for using certain groups of bacteria (endophytic bacteria) for treating UC.

Unedited

5 Conclusions

Our investigation revealed that *R. aegyptiacum* as an endophytic bacterium can effectively restore the normal conditions of colonic mucosa after inducing ulcer through the administration of AA in UC rats. Most importantly, we demonstrated for the first time that *R. aegyptiacum* possesses antioxidant and anti-inflammatory properties. Future studies are required to endorse the clinical use of *R. aegyptiacum* in managing human UC patients.

Data availability statement

All data are available in the manuscript and the supporting material

Acknowledgments

Not applicable

Author contribution

Engy Elekhnawy, Duaa Eliwa, Sarah Ibrahim, Asmaa Ramadan Azzam, and Walaa A. Negm performed the experimental research and data analysis and wrote and edited the manuscript. Sebaey Mahgoub, Sameh Magdeldin, Ehssan Moglad, and Rehab Ahmed contributed to the study design, data analysis, writing and editing of the manuscript. All authors read and approved the final manuscript and, therefore, had full access to all the data in the study and took responsibility for the integrity and security of the data.

Compliance with ethics guidelines

Engy Elekhnawy, Duaa Eliwa, Sebaey Mahgoub, Sameh Magdeldin, Ehssan Moglad, Sarah Ibrahim, Asmaa Ramadan Azzam, Rehab Ahmed, and Walaa A. Negm declare that they have no conflict of interest.

All procedures followed were in accordance with the ethical standards of the responsible committee on human experimentation (Medical Research Ethics Committee, Faculty of Medicine, Tanta University, Egypt with an approval number 36264PR357/9/23) and with the Helsinki Declaration of 1975, as revised in 2008.

Unedited

References

Abdallah HMI, Ammar NM, Abdelhameed MF, Gendy AEGE, Ragab TIM, Abd-ElGawad AM, Farag MA, Alwahibi MS, Elshamy AI, 2020. Protective Mechanism of Acacia saligna Butanol Extract and Its Nano-Formulations against Ulcerative Colitis in Rats as Revealed via Biochemical and Metabolomic Assays. *Biology (Basel)*, 30;9(8):195. https://doi.org/10.3390/biology9080195.

Abdelaziz A, Sonbol F, Elbanna T, El-Ekhnawy E, 2019. Exposure to Sublethal Concentrations of Benzalkonium Chloride Induces Antimicrobial Resistance and Cellular Changes in Klebsiellae pneumoniae Clinical Isolates. *Microb Drug Resist*, 25(5):631-638. https://doi.org/10.1089/mdr.2018.0235.

Adamina M, Feakins R, Iacucci M, Spinelli A, Cannatelli R, D'Hoore A, Driessen A, Katsanos K, Mookhoek A, Myrelid P, Pellino G, Peros G, Tontini GE, Tripathi M, Yanai H, Svrcek M, 2021. ECCO Topical Review Optimising Reporting in Surgery, Endoscopy, and Histopathology. *J Crohns Colitis*, 5;15(7):1089-1105. https://doi.org/10.1093/ecco-jcc/jjab011.

Alherz FA, Negm WA, Elekhnawy E, El-Masry TA, Haggag EM, Alqahtani MJ, Hussein IA, 2022. Silver Nanoparticles Prepared Using Encephalartos laurentianus De Wild Leaf Extract Have Inhibitory Activity against Candida albicans Clinical Isolates. *J Fungi (Basel*), S25;8(10):1005. https://doi.org/ https://doi.org/10.3390/jof8101005.

Almukainzi M, El-Masry TA, Negm WA, Elekhnawy E, Saleh A, Sayed AE, Ahmed HM, Abdelkader DH, 2022. Co-delivery of gentiopicroside and thymoquinone using electrospun m-PEG/PVP nanofibers: In-vitro and In vivo studies for antibacterial wound dressing in diabetic rats. *Int J Pharm*, 25;625:122106. https://doi.org/10.1016/j.ijpharm.2022.122106.

Alotaibi B, El-Masry TA, Elekhnawy E, El-Kadem AH, Saleh A, Negm WA, Abdelkader DH, 2022. Aqueous core epigallocatechin gallate PLGA nanocapsules: characterization, antibacterial activity against uropathogens, and in vivo reno-protective effect in cisplatin induced nephrotoxicity. *Drug Deliv*, 29(1):1848-1862. https://doi.org/10.1080/10717544.2022.2083725.

Ansari MN, Rehman NU, Karim A, Soliman GA, Ganaie MA, Raish M, Hamad AM, 2021. Role of Oxidative Stress and Inflammatory Cytokines (TNF-α and IL-6) in Acetic Acid-Induced Ulcerative Colitis in Rats: Ameliorated by *Otostegia fruticosa*. *Life (Basel*), 3;11(3):195. https://doi.org/10.3390/life11030195.

Attallah NGM, El-Sherbeni SA, El-Kadem AH, Elekhnawy E, El-Masry TA, Elmongy EI, Altwaijry N, Negm WA, 2022a. Elucidation of the Metabolite Profile of Yucca gigantea and Assessment of Its Cytotoxic, Antimicrobial, and Anti-Inflammatory Activities. *Molecules*,16;27(4):1329. https://doi.org/10.3390/molecules27041329.

Attallah NGM, Al-Fakhrany OM, Elekhnawy E, Hussein IA, Shaldam MA, Altwaijry N, Alqahtani MJ, Negm WA, 2022b. Anti-Biofilm and Antibacterial Activities of Cycas media R. Br Secondary Metabolites: In Silico, In Vitro, and In Vivo Approaches. *Antibiotics (Basel)*, 24;11(8):993. https://doi.org/10.3390/antibiotics11080993.

Aziz N, Kim MY, Cho JY, 2018. Anti-inflammatory effects of luteolin: A review of in vitro, in vivo, and in silico studies. *J Ethnopharmacol*, 28;225:342-358.

https://doi.org/10.1016/j.jep.2018.05.019.
Bancroft J D, Gamble M, 2008. Theory and practice of histological techniques, Elsevier health sciences.
Ben-Horin S, Novack L, Mao R, Guo J, Zhao Y, Sergienko R, Zhang J, Kobayashi T, Hibi T, Chowers Y, Peyrin-Biroulet L, Colombel JF, Kaplan GG, Chen MH, 2022. Efficacy of Biologic Drugs in Short-Duration Versus Long-Duration Inflammatory Bowel Disease: A Systematic Review and an Individual-Patient Data Meta-Analysis of Randomized Controlled Trials. *Gastroenterology*. 162(2):482-494.
https://doi.org/10.1053/j.gastro.2021.10.037.
Bertevello PL, Logullo AF, Nonogaki S, Campos FM, Chiferi V, Alves CC, Torrinhas RS, Gama-Rodrigues JJ, Waitzberg DL, 2005. Immunohistochemical assessment of mucosal cytokine profile in acetic acid experimental colitis. *Clinics (Sao Paulo)*, 60(4):277-86.
https://doi.org/10.1590/s1807-59322005000400004.
Blacher E, Levy M, Tatirovsky E, Elinav E, 2017. Microbiome-Modulated Metabolites at the Interface of Host Immunity. *J Immunol*, 15;198(2):572-580.
https://doi.org/10.4049/jimmunol.1601247.
Bruscoli S, Febo M, Riccardi C, Migliorati G, 2021. Glucocorticoid Therapy in Inflammatory Bowel Disease: Mechanisms and Clinical Practice. *Front Immunol*, 3;12:691480.
https://doi.org/10.3389/fimmu.2021.691480.
Checa J, Aran JM, 2020. Reactive Oxygen Species: Drivers of Physiological and Pathological Processes. *J Inflamm Res*, 2;13:1057-1073.
https://doi.org/10.2147/JIR.S275595.
Dignass A, Eliakim R, Magro F, Maaser C, Chowers Y, Geboes K, Mantzaris G, Reinisch W, Colombel JF, Vermeire S, Travis S, Lindsay JO, Van Assche G, 2012. Second European evidence-based consensus on the diagnosis and management of ulcerative colitis part 1: definitions and diagnosis. *J Crohns Colitis*, 6(10):965-90.
https://doi.org/10.1016/j.crohns.2012.09.003.
Elekhnawy E, Negm WA. 2022. The potential application of probiotics for the prevention and treatment of COVID-19. *Egypt J Med Hum Gen*, 23(1):1-9.
https://doi: 10.1186/s43042-022-00252-6
Elmongy EI, Negm WA, Elekhnawy E, El-Masry TA, Attallah NGM, Altwaijry N, Batiha GE, El-Sherbeni SA, 2022. Antidiarrheal and Antibacterial Activities of Monterey Cypress Phytochemicals: In Vivo and In Vitro Approach. *Molecules*, 6;27(2):346.
https://doi.org/10.3390/molecules27020346.
Fan M, Xiang G, Chen J, Gao J, Xue W, Wang Y, Li W, Zhou L, Jiao R, Shen Y, Xu Q, 2020. Libertellenone M, a diterpene derived from an endophytic fungus Phomopsis sp. S12, protects against DSS-induced colitis via inhibiting both nuclear translocation of NF-κB and NLRP3 inflammasome activation. *Int Immunopharmacol*, 80:106144.
https://doi.org/ 10.1016/j.intimp.2019.106144.
Gautam MK, Goel S, Ghatule RR, Singh A, Nath G, Goel RK, 2013 . Curative effect of Terminalia chebula extract on acetic acid-induced experimental colitis: role of antioxidants, free radicals and acute inflammatory marker. *Inflammopharmacology*, 21(5):377-83.
https://doi.org/10.1007/s10787-012-0147-3.
Hsiao YP, Chen HL, Tsai JN, Lin MY, Liao JW, Wei MS, Ko JL, Ou CC, 2021. Administration of Lactobacillus reuteri Combined with Clostridium butyricum Attenuates Cisplatin-Induced Renal Damage by Gut Microbiota Reconstitution, Increasing Butyric Acid Production, and Suppressing Renal Inflammation. *Nutrients*, 15;13(8):2792.
https://doi.org/10.3390/nu13082792.
Kaur L, Gordon M, Baines PA, Iheozor-Ejiofor Z, Sinopoulou V, Akobeng AK, 2020. Probiotics for induction of remission in ulcerative colitis. Cochrane Database Syst Rev, 4;3(3):CD005573.
https://doi.org/10.1002/14651858.CD005573.

Khairy H, Saleh H, Badr AM, Marie MS, 2018. Therapeutic efficacy of osthole against dinitrobenzene sulphonic acid induced-colitis in rats. *Biomed Pharmacother*, 100:42-51.
https://doi.org/10.1016/j.biopha.2018.01.104.
Khare T, Palakurthi SS, Shah BM, Palakurthi S, Khare S, 2020. Natural Product-Based Nanomedicine in Treatment of Inflammatory Bowel Disease. *Int J Mol Sci*, 31;21(11):3956.
https://doi.org/10.3390/ijms21113956.
Lane D, 1991. 16S/23S rRNA sequencing, Nucleic acid techniques in bacterial systematics.
Lavelle A, Sokol H, 2020. Gut microbiota-derived metabolites as key actors in inflammatory bowel disease. *Nat Rev Gastroenterol Hepatol*,17(4):223-237.
https://doi.org/10.1038/s41575-019-0258-z.
Le Loupp AG, Bach-Ngohou K, Bourreille A, Boudin H, Rolli-Derkinderen M, Denis MG, Neunlist M, Masson D, 2015. Activation of the prostaglandin D2 metabolic pathway in Crohn's disease: involvement of the enteric nervous system. *BMC Gastroenterol*, 4;15:112.
https://doi.org/10.1186/s12876-015-0338-7.

unedited

Li X, Liu X, Zhang Y, Zhang Y, Liu S, Zhang N, Li Y, Wang D, 2020. Protective effect of Gloeostereum incarnatum on ulcerative colitis via modulation of Nrf2/NF-κB signaling in C57BL/6 mice. Mol Med Rep, 22(4):3418-3428. https://doi.org/10.3892/mmr.2020.11420.

Liu Y, Wei W, Liang S, Fang H, Cao J, 2022. Esculentoside A could attenuate apoptosis and inflammation in TNBS-induced ulcerative colitis via inhibiting the nuclear translocation of NF-κB. *Ann Transl Med*,10(14):771. https://doi.org/10.21037/atm-22-2675.

Liu, Xiaoli et al., 2007. Antioxidant activity and phenolics of an endophytic Xylaria sp. from Ginkgo biloba. *Food Chemistry*, 105: 548-554. https://doi.org/10.1016/j.foodchem.2007.04.008.

Livak KJ, Schmittgen TD, 2001. Analysis of relative gene expression data using real-time quantitative PCR and the 2(-Delta Delta C(T)) Method. *Methods*, 25(4):402-8. https://doi.org/10.1006/meth.2001.1262.

Mi H, Liu FB, Li HW, Hou JT, Li PW, 2017. Anti-inflammatory effect of Chang-An-Shuan on TNBS-induced experimental colitis in rats. *BMC Complement Altern Med*, 15;17(1):315. https://doi.org/10.1186/s12906-017-1794-0.

Quettier-Deleu C, Gressier B, Vasseur J, Dine T, Brunet C, Luyckx M, Cazin M, Cazin JC, Bailleul F, Trotin F, 2000. Phenolic compounds and antioxidant activities of buckwheat (Fagopyrum esculentum Moench) hulls and flour. *J Ethnopharmacol*, 72(1-2):35-42. https://doi.org/10.1016/s0378-8741(00)00196-3.

Raish M, Shahid M, Bin Jardan YA, Ansari MA, Alkharfy KM, Ahad A, Abdelrahman IA, Ahmad A, Al-Jenoobi FI, 2021. Gastroprotective Effect of Sinapic Acid on Ethanol-Induced Gastric Ulcers in Rats: Involvement of Nrf2/HO-1 and NF-κB Signaling and Antiapoptotic Role. *Front Pharmacol*, 25;12:622815. https://doi.org/10.3389/fphar.2021.622815.

Ran ZH, Chen C, Xiao SD, 2008. Epigallocatechin-3-gallate ameliorates rats colitis induced by acetic acid. Biomed Pharmacother, 62(3):189-96. https://doi.org/10.1016/j.biopha.2008.02.002.

Rana KL, Kour D, Kaur T, Devi R, Yadav AN, Yadav N, Dhaliwal HS, Saxena AK, 2020. Endophytic microbes: biodiversity, plant growth-promoting mechanisms and potential applications for agricultural sustainability. *Antonie Van Leeuwenhoek*, 113(8):1075-1107. https://doi.org/10.1007/s10482-020-01429-y.

Peyrottes A, Coquant G, Brot L, Rainteau D, Seksik P, Grill JP, Mallet JM. Anti-Inflammatory Effects of Analogues of *N*-Acyl Homoserine Lactones on Eukaryotic Cells. Int J Mol Sci. 2020 Dec 11;21(24):9448. https://doi: 10.3390/ijms21249448.

Piechota-Polanczyk A, Fichna J, 2014 .Review article: the role of oxidative stress in pathogenesis and treatment of inflammatory bowel diseases. *Naunyn Schmiedebergs Arch Pharmacol*, 387(7):605-20. https://doi.org/10.1007/s00210-014-0985-1.

Popov J, Caputi V, Nandeesha N, Rodriguez DA, Pai N, 2021. Microbiota-Immune Interactions in Ulcerative Colitis and Colitis Associated Cancer and Emerging Microbiota-Based Therapies. Int J Mol Sci, Oct 21;22(21):11365. http://doi.org/10.3390/ijms222111365.

Singh M, Kumar A, Singh R, Pandey KD, 2017. Endophytic bacteria: a new source of bioactive compounds. 3 *Biotech*, 7(5):315. https://doi.org/10.1007/s13205-017-0942-z.

Shahid M, Raish M, Ahmad A, Bin Jardan YA, Ansari MA, Ahad A, Alkharfy KM, Alaofi AL, Al-Jenoobi FI, 2022. Sinapic Acid Ameliorates Acetic Acid-Induced Ulcerative Colitis in Rats by Suppressing Inflammation, Oxidative Stress, and Apoptosis. *Molecules*, 28;27(13):4139. https://doi.org/10.3390/molecules27134139.

Strobel G, Daisy B, 2003. Bioprospecting for microbial endophytes and their natural products. *Microbiol Mol Biol Rev*, 67(4):491-502. https://doi.org/10.1128/MMBR.67.4.491-502.2003.

Telesford KM, Yan W, Ochoa-Reparaz J, Pant A, Kircher C, Christy MA, Begum-Haque S, Kasper DL, Kasper LH, 2015. A commensal symbiotic factor derived from Bacteroides fragilis promotes human CD39(+)Foxp3(+) T cells and Treg function. *Gut Microbes*, 4;6(4):234-42. https://doi.org/10.1080/19490976.2015.1056973.

Twaij BM, Hasan MN, 2022. Bioactive Secondary Metabolites from Plant Sources: Types, Synthesis, and Their Therapeutic Uses. *International Journal of Plant Biology*,13(1):4-14. https://doi.org/10.3390/ijpb13010003.

Vavricka SR, Brun L, Ballabeni P, Pittet V, Prinz Vavricka BM, Zeitz J, Rogler G, Schoepfer AM, 2011. Frequency and risk factors for extraintestinal manifestations in the Swiss inflammatory bowel disease cohort. *Am J Gastroenterol*, 106 (1):110-9. http://doi.org/10.1038/ajg.2010.343.

Wang Q. et al., 2021. Potential anti-inflammatory activity of walnut protein derived peptide leucine-proline-phenylalanine in lipopolysaccharides-irritated RAW264.7 cells. *Food and Agricultural Immunology*, 32(1): 663 - 678. https://doi.org/10.1080/09540105.2021.1982870.

Wang D, Dubois RN, 2010. The role of COX-2 in intestinal inflammation and colorectal cancer. *Oncogene*, 11;29 (6):781-8.

Unedited

https://doi.org/10.1038/onc.2009.421.
Xue JC, Yuan S, Hou XT, Meng H, Liu BH, Cheng WW, Zhao M, Li HB, Guo XF, Di C, Li MJ, Zhang QG, 2023. Natural products modulate NLRP3 in ulcerative colitis. *Front Pharmacol*, 2;14:1265825.
https://doi.org/10.3389/fphar.2023.1265825.

Supplementary information

Table S1; Materials and methods; Figs. S1-S3; Results

unedited